ELSEVIER

Colloids and Surfaces
A: Physicochemical and Engineering Aspects 183–185 (2001) 113–122

COLLOIDS AND SURFACES A

www.elsevier.nl/locate/colsurfa

Digital cryogenic transmission electron microscopy: an advanced tool for direct imaging of complex fluids

D. Danino [1], A. Bernheim-Groswasser, Y. Talmon *

Department of Chemical Engineering, Technion – Israel Institute of Technology, Haifa 32000, Israel

Abstract

Digital imaging cryogenic transmission electron microscopy (cryo-TEM) has become an important extension of TEM at cryogenic temperatures. In this paper, we describe the advantages of the technique and demonstrate its use in the study of two micellar systems. We show how details that were impossible or difficult to image, can be easily observed by this novel technique. We emphasize that the introduction of digital imaging to cryo-TEM is not merely a small technical improvement, but does promise to expand the capabilities of TEM of complex fluids in a most significant way. © 2001 Elsevier Science B.V. All rights reserved.

Keywords: Cryogenic-transmission electron microscopy; Micelles; Micellar junctions; Micellar end-caps; Networks

1. Preface

Professor Heinz Hoffmann has been, for many years now, one of the advocates and practitioners of transmission electron microscopy. Naturally he has always combined his microscopy with many other (indirect!) techniques. Most of his excellent microscopy work has been done by applying freeze-fracture-replication TEM in the study of a wide range of systems. In that respect our groups have complemented each other, as we have used over the years mostly direct imaging cryo-TEM. The paper that follows describes the very significant progress that has been made in expanding the applicability of cryo-TEM to many systems not approachable by the technique before, and making many details that had been thought to be ''invisible'' – visible. To a large extent this has been made possible by combining digital imaging with cryo-TEM. While to some, this may seem a mere ''technical improvement'', it has, in fact, taken cryo-TEM as applied to complex fluids a giant step forward. In what follows we give some background to the subject, and explain in detail the limitations of cryo-TEM (to which we were accustomed until recently, and conducted our work accordingly), and the ways that digital imaging has made it possible to overcome some of those limitations. As will be emphasized, it takes retraining and using a fresh approach to TEM as applied to complex fluids in order to take advan-

* Corresponding author. Tel.: +972-4-8292820; fax: +972-4-8230476.

E-mail address: ishi@techunix.technion.ac.il (Y. Talmon).

[1] Laboratory of Cell Biochemistry and Biology, Building 8, Room 419, 8 Center Dr., NIDDK, NIH, Bethesda, MD 20892, USA.

0927-7757/01/$ - see front matter © 2001 Elsevier Science B.V. All rights reserved.
PII: S0927-7757(01)00543-X

tage of this technological breakthrough. This paper is dedicated to Professor Heinz Hoffman on the occasion of his 65th birthday, as a small token of our deep appreciation of his scientific achievements.

2. Introduction

Amphiphilic molecules spontaneously self-associate into micelles when dispersed in solvents above the critical micellization concentration (CMC). Just above this concentration, micelles are generally spherical or spheroidal [1]. With change of a control parameter such as surfactant concentration [2], salinity [3,4] or temperature [5], micelles often grow into elongated, locally cylindrical, micelles that can become extremely long [6]. Such micelles have been referred to as 'threadlike' [7] micelles. Further change in the control parameter may lead to transitions into structures of lower curvature such as ribbons [8–10], discs [11,12], and vesicles [13], or to formation of ordered liquid crystalline phases [14].

Many experimental techniques have been used to study the microstructures of micellar solutions and other complex fluids. Self-diffusion NMR [15], fluorescence [16], and scattering techniques such as small-angle neutron (SANS) [17,18], X-ray (SAXS) [19], and light scattering (static and dynamic) [20,21] provide microstructural information on the size, shape, and interactions that govern spatial organization. However, these techniques are all considered indirect, as they require predetermined models for data interpretation. In addition, the information provided is not of a single aggregate, but is averaged over all sample volume. Interpretation of data becomes extremely difficult in the case of coexistence of structures of different size or topology.

Detailed and aggregate-specific information about microstructured fluids can be obtained from direct imaging techniques, such as light microscopy and transmission electron microscopy (TEM). In particular, direct imaging cryogenic TEM (cryo-TEM) [22–24] has become indispensable in the study of diverse systems such as surfactant, polymer and polymer-surfactant solutions, and microemulsions, as well as biological and biomedical systems. For aggregates in the size range of 1–300 nm[2], information of the exact shape of a single particle and coexistence of very different structures can be readily obtained. The study of those systems has become more feasible and effective with technological developments of today's microscopes. In particular, digital imaging cryo-TEM has overcome some of the difficulties encountered previously using photographic film, as is discussed below.

3. Digital imaging transmission electron microscopy

Until recently, TEM images were usually recorded on photographic film based on silver halide emulsions. Images have been recorded typically by direct exposure of the film to the electron beam. While the film has reasonably good grain size and quantum efficiency, it has a rather limited linear response range [25]. The film as received from the manufacture is "wet", i.e., contains much volatile material. It takes elaborate prepumping to remove those volatiles to an acceptable level. In addition, removal of exposed film from the microscope camera and introduction of fresh film cause some deterioration of the high vacuum (in the range of 10^{-5} Pa in modern TEMs) in the microscope. If the use of photographic film is avoided, the quality of the microscope vacuum (absolute pressure and residual gas composition) is much improved. This is of particular significance when cryo-TEM is applied, as the low-temperature specimen may act as a cryopump, collecting condensed volatiles on its surfaces. Those deposits interfere with imaging, and in some cases may be confused for real microstructures.

[2] The desirable thickness of a cryo-TEM specimen for the most commonly used 120 kV electron microscope is less than 300 nm. However, objects larger in one (e.g., threadlike micelles) or two (e.g., membrane sheets) dimensions can also be easily examined, as they tend to accommodate themselves in the relatively thin liquid specimen prior to vitrification. In some cases, objects quite large in all three dimensions (such as large liposomes) are flattened during specimen preparation and thus can be imaged by cryo-TEM.

The progress in charge-coupled device (CCD) cameras has made it possible to make the technology available for TEM imaging [26]. In this case, the electron beam hits a scintillating layer on the detector, and the image is usually recorded by an array of 1024×1024 pixels. Detectors twice as big are also commercially available now. In addition to dispensing with films, CCD cameras offer several other advantages that are most important for cryo-TEM work. The first advantage is the ability of CCD cameras to record images at very low electron exposure. This is of paramount importance for typical complex fluids cryo-specimens which are extremely sensitive to the electron beam [27]. While those images are of rather poor signal-to-noise ratio, they provide sufficient information for the selection of suitable areas for taking micrographs, and to adjust the microscope parameters for optimal imaging. Without a CCD camera, one cannot preview the image, and has to "shoot in the dark" in hope the negatives developed later in the dark room do provide the information needed. In addition, because of the high sensitivity of the detectors, one can now go to microscope magnifications that are much higher than what was possible before, without significant deleterious effects. While most images are recorded on film at a magnification of 20 000–30 000 times, with the CCD camera we are able to take micrographs at a magnification of 140 000 times and higher, thus obtaining higher resolution.

Another important aspect of digital imaging is the ease of real-time and post-microscopy image processing. This is most significant when recording images of vitrified complex fluids that, due to their composition, have inherently very low contrast. Even simple operations such as background subtraction (the subtraction of the average local signals or 'DC level'), or contrast and brightness enhancement can bring out details otherwise too faint to detect. A clear illustration of this advantage is the ability of digital imaging cryo-TEM to reveal both the corona and the core parts of diblock copolymer micelles [28], while previous attempts to detect the corona on film had failed. The corona part is made of poly(ethyleneoxide), thus it has very little contrast relative to the surrounding vitrified water.

Finally, it should be mentioned that collecting images as computer files makes it easy to share the information, and to archive and retrieve it. The latter operations require special attention for backing-up the data and computer-based cataloging.

In what follows, we describe the application of digital cryo-TEM to several micellar systems with emphasis on special features that have been made visible by the technique. Technical details relating to the application of this approach are given, and issues of contrast are discussed.

4. Experimental

4.1. Materials

Habon G, a commercial surfactant mixture of 53.5 wt.% hexadecylhydroxyethyl-dimethylammonium-3,2 hydroxy naphthoate, 10.2% isopropanol and 36.3% water, was dissolved in water to a final concentration of 0.1 wt.% of active surfactant at 20°C. The solution was obtained from Prof. G. Hetsroni of the Department of Mechanical Engineering, Technion, as part of an ongoing project [29].

The hybrid gemini surfactant '$C_8^F C_4$-2-12', in which some of the hydrogen atoms on one of the dodecyl chains were substituted by fluorine atoms was synthesized by Dr. I. Huc (Institut Européen de Chimie et Biologie, Talence Cedex, France). Aqueous solutions of this surfactant were provided by Dr. R. Oda also of the Institut Européen de Chimie et Biologie [30].

4.2. Cryo-transmission electron microscopy

Specimens were prepared in a controlled environment vitrification system (CEVS) at controlled temperature and humidity to avoid loss of volatiles [22]. A drop of the examined solution was placed on a TEM grid covered by a perforated carbon film. The drop was then blotted with a filter paper to form a thin liquid film on the grid, and immediately plunged into liquid ethane at its freezing temperature (-183°C). The vitrified specimens were stored under liquid nitrogen

(−196°C) and observed in a Philips CM120 transmission electron microscope optimized for cryo-TEM work. The microscope was operated at an accelerating voltage of 120 kV. We used an Oxford CT3500 cryo-specimen holder that maintained the vitrified specimens below −175°C. Specimens were examined in the low-dose imaging mode to minimize electron-beam radiation damage. Images at nominal magnifications up to 175 000 times were recorded digitally by a Gatan MultiScan 791 CCD camera at appropriate objective lens underfocus conditions (2–4 μm) to enhance phase-contrast, using the Digital Micrograph 3.1 software package.

General areas of interest were selected at low magnification (usually 3400×) using the TV rate scan of the camera. Appropriate areas for microscopy were selected at moderate magnifications (typically 53 000×) and very low electron exposure. Focusing conditions were also established at those magnifications, taking into account the difference in focus setting between the lower and higher (final) magnification. This procedure allowed us to obtain a high yield of usable images with exposures ('electron doses') less than 20 electrons per Å^2. At those electron exposures no apparent damage to the specimen was observed, while doubling the exposure often produced damage to the finer structural details and to the perforated carbon support film.

5. Results and discussion

High resolution details can be detected when working at high magnifications, focusing on aggregates of choice, and adjusting imaging conditions, such as objective lens underfocus and electron dose for acceptable signal-to-noise ratio, while minimizing electron-beam radiation-damage. Fine microstructural details of threadlike micelles are demonstrated in Fig. 1, a cryo-TEM digital image of 0.1 wt.% Habon G aqueous solution. The first striking fact is that threadlike micelles are not imaged here as one-dimensional lines, but show quite clearly finite thickness and diameter variation along the micelle. Indeed, such images indicate clearly that threadlike micelles are not the perfect curved cylinders often shown in artist renditions of those aggregates. Undulations along the micelles are also observed quite clearly, as, for example, in the lower right side of Fig. 1(A). In that particular image there is no preferred orientation of the micelles shown in the field of view, indicating that the effects of the shear during specimen preparation [31] have relaxed. In Fig. 1, we can also easily distinguish between crossover of two micelles and junction or branching points. A typical case of two superposed crossing micelles is indicated in Fig. 1(A) by an arrowhead and magnified by a factor of two in Fig. 1(B). Note the dark square that is formed in the image of the areas of overlap of the two micelles. A junction in Fig. 1(A) is indicated by a black arrow and is magnified 2× in Fig. 1(C). While junctions have been shown already by cryo-TEM some years ago [32], here we can see for the first time the inner structure of the junctions. A second junction is seen right of the center of Fig.

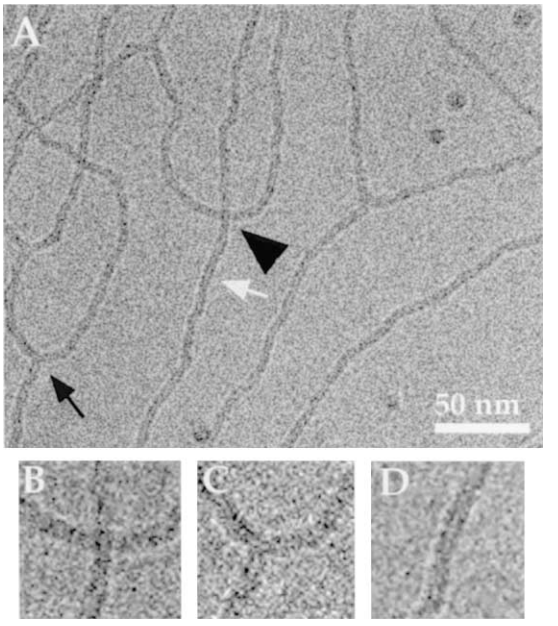

Fig. 1. (A) High magnification image of threadlike micelles observed in a vitrified 0.1 wt.% Habon G solution quenched from 20°C. Arrowhead points to two overlapping micelles, enlarged ×2 in (B). Black arrow indicates a branching point enlarged ×2 in (C). White arrow points to a section of a micelle, enlarged ×2 in (D).

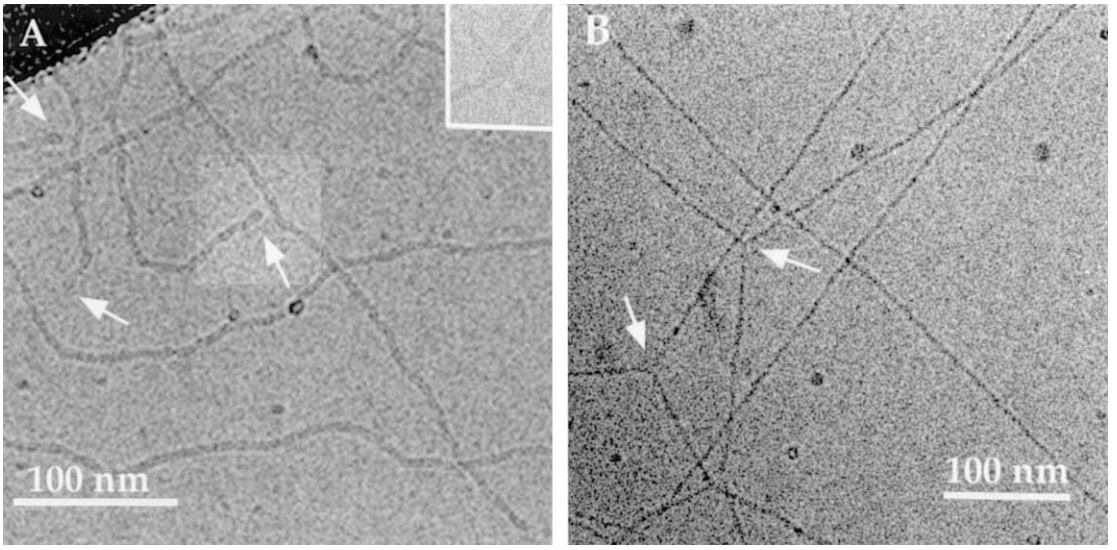

Fig. 2. (A) Swollen end-caps (arrows) of threadlike micelles imaged in a vitrified 0.1 wt.% Habon G solution quenched from 20°C. The center of the image has been processed separately to bring out the details of the end-cap, almost touching another micelle. The inset (50 nm wide) shows a four-micelle junction. (B) Lower magnification image showing a sparse network of micelles. Arrows mark three-fold junctions, with 120° angles between micelles.

1(A). Finally, high magnification images such as Fig. 1(A) show contrast features that require some discussion. Some domains along the micelles length show white and dark line parallel to the micelle long axis. An example is indicated by a white arrow in Fig. 1(A) and is shown magnified in Fig. 1(D). Because the objective lens of the TEM is underfocused (see above) to enhance phase contrast (see, for example, Misell [33]), a Fresnel fringe is observed at the edge of the micelles where the density changes abruptly from that of water to that of the head-groups of the micelles. The fringe is light in the lower density region and dark in the high density domain. Curiously, however, the dark fringe is very non-uniform, suggesting possible density fluctuations along the micelles. Now that cryo-TEM imaging has been pushed that far, this particular issue of density fluctuations along and across the micelle should be studied more carefully in the future, especially in micellar system of different atomic (or molecular) weight counter-ions and different degrees of surfactant ionization.

Another feature that has now been imaged by cryo-TEM is the end-caps of threadlike micelle. Elongated micelles had been assumed to be spherocylindrical, i.e., cylinders terminated by hemispherical end-caps of the same diameter as that of the cylinder core [1]. However, other models [34–36] suggested that the end-caps are swollen, i.e., of larger diameter than that of the cylindrical body. The cryo-TEM image of 0.1 wt.% Habon G aqueous solution presented in Fig. 2(A) shows several elongated micelles ending in swollen end-caps (arrows). The center of Fig. 2(A) (a square somewhat lighter than the rest of the micrograph) was processed differently to bring out the details of an end-cap, that is near, but not touching another threadlike micelle. These images of swollen end-caps should not be confused with the occasional appearance of a darker spot at the end of threadlike micelles (see an early report by Claussen et al. [37]). That effect is due to the occasional orientation of the micelle end-segment parallel to the electron beam. Here, the situation is quite different, as the average optical density of the end-cap is the same as that of the main body of the micelle. Because the image is recorded digitally, optical density is easily measurable down to the single pixel level! Because of its large

molecule and the bulky counter-ion, the images of end-caps of Habon G are rather clear. Imaging is more difficult in other systems such as the gemini surfactant 12-2-12 [38]. The end-cap is more easily imaged by digital cryo-TEM in the much lager polymer micelles, where the end-cap is shown complete with its corona [28]. All those observations support the above mentioned models suggesting swollen end-caps.

When end-caps become energetically unfavorable, elongated micelles interconnect via junctions to form branched networks. Interconnected micelles were suggested by Porte et al. more than a decade ago [39], and later proposed theoretically by Drye and Cates [40] and by Bohbot et al. [41]. As mentioned above, we observed branched micelles by cryo-TEM and identified them for the first time just a few years ago [32], confirming unambiguously their existence. At that time, it was assumed that only certain surfactants could form such junctions of 'special' saddle-like curvatures. Now it is known to be a more general property, identified in many systems [37,42,43]. With today's advanced technology, we can distinguish between different types of junctions and learn about their structure. Three-fold junctions have been discussed above. In most cases the angles between micelles are close to 120° as was proposed theoretically [44,45]. This is also seen in the micelles of Fig. 1. When the micelles are rigid (Fig. 2(B)) this angle persists to several micrometers. This is demonstrated clearly by Fig. 2(B), where the arrows point to the junctions. Four-fold junctions also form and are imaged now routinely, but less frequently than three-fold ones. The inset in Fig. 2(A) shows clearly a four-fold junction that seems to be locally flat (as deduced from the little variation of optical density across the junction domain), with an angle of about 90° between any two adjacent micelles. Naturally, to be able to focus on specific microstructure, such as the sparse network in Fig. 2(B), digital imaging is indispensable. Large areas of cryo-TEM specimens lack interesting features. The ability to prescreen areas for different microstructures, expected or unexpected, is an outstanding advantage of the technique.

It is now quite well established that cryo-TEM is most useful for identifying the shape of single particles and observing the coexistence of aggregates of different topologies, as well as revealing peculiar intermediates and defects in the aggregate structure. When 'shooting in the dark', i.e., when taking micrographs without actually seeing the target area, as one does when not using digital imaging, it is exceedingly difficult to acquire the needed information, especially when one is hunting for a particular feature. Also the inherent low contrast in vitrified specimens of complex fluids makes it quite difficult to actually see that sought after feature, even if it is actually in the field of view. Those problems are overcome to a large extent by using digital imaging cryo-TEM, as illustrated by Fig. 3. In a 3.0 wt.% solution of the $C_8^FC_4$-2-12 gemini surfactant, three-fold junctions connecting thin ribbon-like structures were successfully identified and observed. These features are shown in Fig. 3(A) marked by arrows. In contrast to three-fold junctions of threadlike micelles, these junctions are locally flat, as may be deduced from their uniform optical density (see inset). The flat appearance is consistent with the general tendency of this system to form structures of low curvature, i.e., vesicles and ribbons and other open bilayers [30]. The latter publication discusses in detail the different microstructures in $C_8^FC_4$-2-12 and related surfactants. The relative contrast between the junction (inset in Fig. 3(A)) and the vitreous ice in the micrograph, as recorded digitally, was measured under 3%, well below the rule-of-thumb threshold value of 5%. However, simple contrast enhancement brings out the required details.

Transition from highly curved cylindrical micelles to flat bilayers can occur via ribbon-like intermediates. Indeed, using digital-imaging cryo-TEM we have been able to capture that transition and the coexistence of threadlike micelles and flat bilayer sheets in a 0.5 wt.% solution of the dimeric surfactant $C_8^FC_4$-2-12. In the micrograph shown in Fig. 3(B) threadlike micelles have been caught in the action of opening into ribbon-like structures of broad width distribution (arrows). This process eventually leads to formation of vesicles, as shown in Fig. 3(A). Intermediate ribbon-like structures

were seen before in a binary system of a gemini surfactant of two different alkyl chains [10]. Helical and twisted ribbons with well-defined pitch and width [9] were also observed in gemini surfactant systems by cryo-TEM. However, digital-imaging cryo-TEM facilitates considerably the scanning of the specimen and searching for the structures in question, provide higher quality micrographs and a much larger number of them for the invested time and effort.

In systems composed of compounds of very different chemical nature, several types of aggregates of different curvature may form simultaneously. Intermediate structures and physical connections between those aggregates can form as a result of fluctuations in local concentration. For instance, if we return now to the Habon G system, we should remember that this surfactant is actually of mixture of two surfactants, the cationic and the anionic moieties, and, in addition, a cosurfactant is also present in that commercial 'detergent'. Due to this mixture we are able to observe in this system not only the features described above and shown in Figs. 1 and 2, but also, quite unexpectedly, vesicles linked by interconnected threadlike micelles (Fig. 4). Some of the connection points between vesicles and micelles, are marked by smaller arrows. The micrograph was taken at a fairly high defocus of 4 micrometers to enhance contrast (this leads to the formation of the very clear light Fresnel fringes around the round vesicles), but even then doubt may remain regarding whether those connections are real or just superposition of images of micelles and vesicles. The micrograph was thus further processed to enhance contrast. Just a small (darker) area in its upper part was left in its original condition to allow comparison between contrast before and after processing. At the improved level of contrast it is easy to tell real connections (small arrows) and a superposition of a micelle and a vesicle (larger arrow). Those unusual threadlike micelle-to lamella junctions are probably formed to avoid energetically unfavorable end-caps. Similar connections were also seen in mixed dimeric surfactants [30]. This is, of course, also the reason for junction or branch formation in threadlike micelles, seen quite clearly here, too, in Fig. 4 (arrowheads).

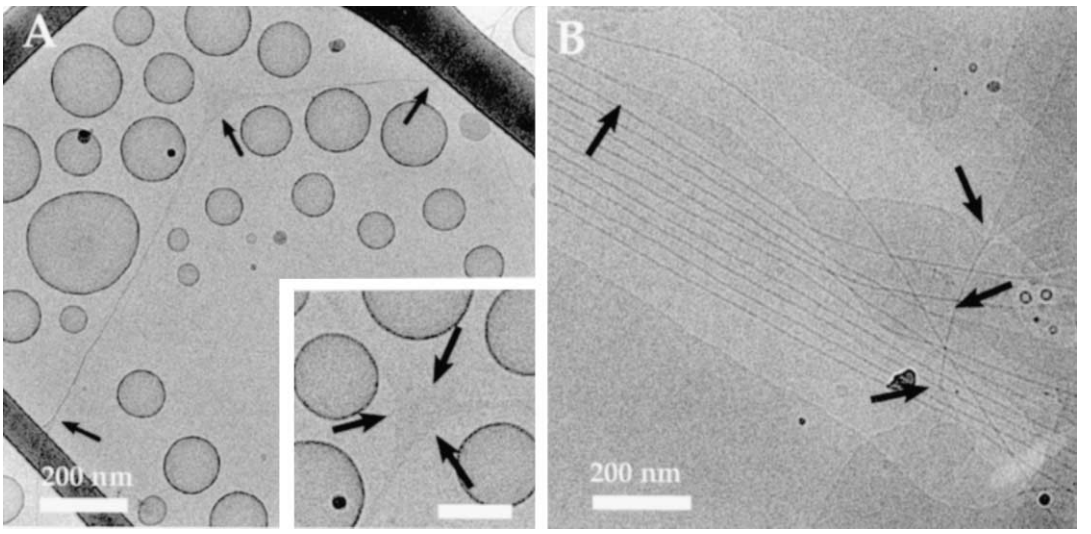

Fig. 3. (A) Cryo-TEM image of a 3 wt.% aqueous solution of the hybrid $C_8^FC_4$-2-12 gemini surfactant showing three-fold locally flat junctions (arrows), connecting ribbon-like structures. Inset shows the upper left junction at a higher magnification (bar = 100 nm). (B) Threadlike micelles that open into ribbon-like structures with broad width distribution (arrows) are found at 0.5 wt.% of $C_8^FC_4$-2-12.

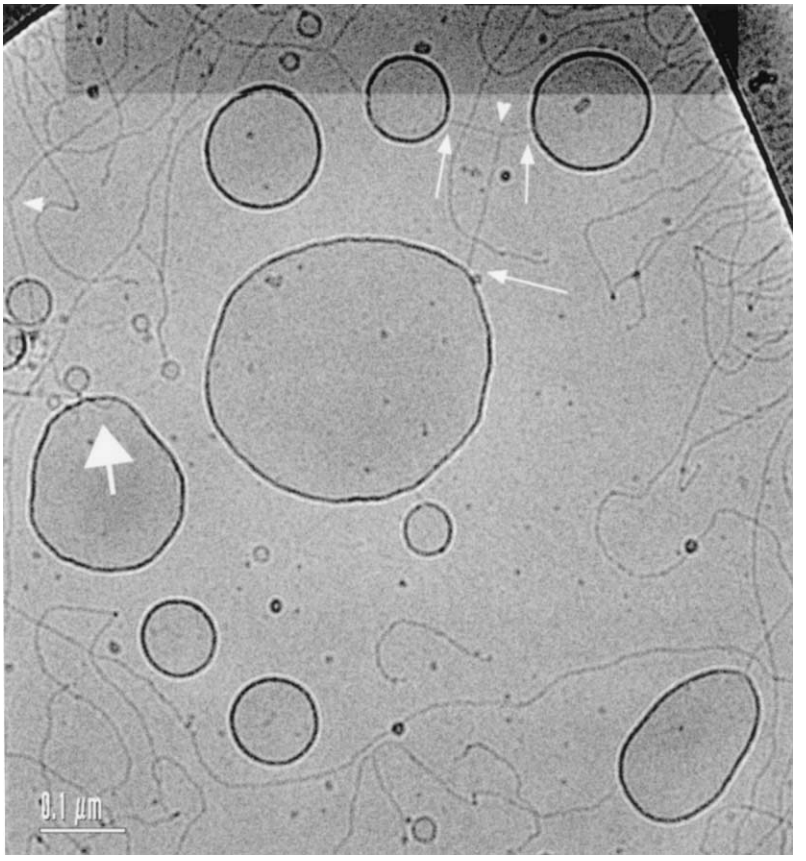

Fig. 4. The coexistence of threadlike micelles and vesicles found in a 0.1 wt.% solution of Habon G at 20°C. Notice three-fold micelle junctions (arrowheads) and micelle–lamella junctions (smaller arrows). The large arrow points to an overlap of a micelle and a vesicle. Most of the image was processed to enhance contrast by 'unsharp masking' background-subtraction. Only a narrow (darker) strip in the upper part was left in the original state for comparison.

6. Conclusions

Digital-imaging cryo-TEM is now available in an increasing number of laboratories. The technique is not a mere extension of cryo-TEM using photographic, but a major technological forward step that opens up many new possibilities, on the one hand, and requires understanding the new capabilities, on the other hand. In fact, for the microscopist, the transition is not straight forward, but requires rethinking the process of experiment design and execution.

The main advantages of digital cryo-TEM are cleaner microscope vacuum (as photographic film is eliminated) to minimize contamination deposition on the sample; the ability to carefully select the target area at low electron exposures; easy low-electron-dose imaging at relatively high magnification that leads to high resolution; easy real-time and post-microscopy image processing; easy distribution of data via communications networks.

In this paper, we have demonstrated some of the benefits that the above mentioned advantages can bring to the study of complex fluids. We have chosen as our demonstration tool threadlike micellar systems that until recently were imaged merely as one-dimensional curved objects. We have shown how inner structural details such as the shape of end-caps and junctions can be imaged, and that image processing can bring out details of very low contrast. It should be empha-

sized that all the images shown above are low-electron-dose images – an integral part of proper digital imaging protocols. That means that minimal high-resolution structural detail is lost to electron beam radiation damage.

Better resolution, improved contrast and lower electron damage allow the study of many system that we were not able to study efficiently before. This includes nonaqueous systems such as oil-continuous microemulsions and microsuspensions, and the application of electron diffraction to study sensitive organic crystals in the hydrated state.

Acknowledgements

This work was supported in part by a 'Center of Excellence' grant from the Israel Science Foundation of the Israel Academy of Sciences and Humanities. The cryo-TEM work was performed at the 'Cryo-TEM Hannah and George Krumholz Laboratory for Advanced Microscopy' at the Technion. The authors wish to thank Profs. G. Hetsroni and J. Zakin, and Drs I. Huc and R. Oda, for providing the compounds used in this study. We thank J. Schmidt and B. Shdemati for excellent technical assistance.

References

[1] J.N. Israelachvili, D.J. Mitchell, B.W. Ninham, J. Chem. Soc. Faraday Trans. II 72 (1976) 1525.
[2] P.G. Missel, N.A. Mazer, G.B. Benedek, C.Y. Young, M. Carey, J. Phys. Chem. 84 (1980) 1044.
[3] B. Kachar, D.F. Evans, B.W. Ninham, J. Colloid Interface Sci. 100 (1984) 287.
[4] G. Porte, J. Marignan, P. Bassereau, R. May, J. de Physique 49 (1988) 511.
[5] V. Degiorgio, in: V. Degiorgio, M. Corti (Eds.), Physics of Amphiphiles: Micelles, Vesicles and Microemulsions, North-Holland, Amesterdam, 1985, p. 303.
[6] G. Porte, J. Appell, J. Phys. Chem. 85 (1981) 2511.
[7] P.K. Vinson, Y. Talmon, J. Colloid Interface Sci. 133 (1989) 288.
[8] M. Bergström, J.S. Pedersen, Langmuir 15 (1999) 2250.
[9] R. Oda, I. Huc, M. Schmutx, S.J. Candau, F.C. MacKintosh, Nature 399 (1999) 566.
[10] R. Oda, I. Huc, J.-C. Homo, B. Heinrich, M. Schmutz, S.J. Candau, Langmuir 15 (1999) 2384.
[11] M. Goldraich, J.R. Schwartz, J.L. Burns, Y. Talmon, Colloids and Surfaces A 125 (1997) 231.
[12] Th. Zemb, M. Dubois, B. Demé, Th. Gulik-Krzywicki, Science 283 (1999) 816.
[13] D. Danino, M. Abe, R. Zana, Y. Talmon, in preparation.
[14] R. Strey, R. Schomacker, D. Roux, F. Nallet, U. Olsson, J. Chem. Soc. Faraday Trans. 86 (1990) 2253.
[15] P.G. Nilsson, H. Wennerström, B. Lindman, J. Phys. Chem. 87 (1983) 1377.
[16] D. Danino, Y. Talmon, R. Zana, J. Colloid Interface Sci. 286 (1997) 170.
[17] Y.Y. Won, H.T. Davis, F.S. Bates, Science 283 (1999) 960.
[18] H. Bagger-Jorgensen, U. Olsson, K. Mortensen, Langmuir 13 (1997) 1413.
[19] J.O. Rädler, I. Koltover, T. Salditt, C.R. Safinya, Science 275 (1997) 810.
[20] E. Buhler, J.P. Munch, S.J. Candau, J. Phys. II France 5 (1995) 765.
[21] M. Almgren, J.C. Gimel, K. Wang, G. Karlsson, K. Edwards, W. Brown, K. Mortensen, J. Colloid Interface Sci. 202 (1998) 222.
[22] Y. Talmon, in: B.P. Binks (Ed.), Modern Characterization Methods of Surfactant Systems, Marcel Dekker, New York, 1999, p. 147.
[23] D. Danino, Y. Talmon, in: A. Baskin, W. Norde (Eds.), Physical Chemistry of Biological Interfaces, Marcel Dekker, New York, 2000, p. 799.
[24] M. Almgren, K. Edwards, J. Gustafsson, Current Opin. Coll. Interface Sci. 1 (1996) 270.
[25] A.W. Agar, R.H. Alderson, D. Chescoe, in: Principles and Practice of Electron Microscope Operation, North-Holland, Amsterdam, 1974 (Chapter 7).
[26] P.E. Mooney, O.L. Krivanek, D.A. Ray, J. Charlesworth, in: G.W. Bailey, J. Bentley, A. Small (Eds.), Proceedings of 50th Annual Meeting of the Microscopy Society of America, 1992, p. 974.
[27] Y. Talmon, in: R.A. Steinbrecht, K. Zierold (Eds.), Cryotechniques in Biological Electron Microscopy, Springer, Berlin, 1987 Chapter 3.
[28] Y. Zheng, Y.-Y. Won, F.S. Bates, H.T. Davis, L.E. Scriven, Y. Talmon, J. Phys. Chem. B 103 (1999) 10331.
[29] G. Hetsroni, Y. Talmon, J.L. Zakin, A. Mosyak ASME J. Heat Transfer, submitted for publication.
[30] R. Oda, I. Huc, D. Danino, Y. Talmon, Langmuir, 16 (2000) 9759.
[31] Y. Zheng, Z. Lin, J. Zakin, L.E. Scriven, H.T. Davis, Y. Talmon, J. Phys. Chem. B 104 (2000) 5263.
[32] D. Danino, Y. Talmon, H. Lévy, G. Beinert, R. Zana, Science 269 (1995) 1420.
[33] D.L. Misell, Image Analysis, Enhancement and Interpretation, North Holland, Amsterdam, 1978.
[34] J.C. Eriksson, S. Ljunggren, J. Chem. Soc. Faraday Trans. II 81 (1985) 1209.

[35] J.C. Eriksson, S. Ljunggren, Langmuir 63 (1990) 895.
[36] G. Porte, Y. Poggi, J. Appell, G. Maret, J. Phys. Chem. 88 (1984) 5713.
[37] T.M. Clausen, P.K. Vinson, J.R. Minter, H.T. Davis, Y. Talmon, W.G. Miller, J. Phys. Chem. 96 (1992) 474.
[38] A. Bernheim-Groswasser, R. Zana, Y. Talmon, J. Phys. Chem. B 104 (2000) 4005.
[39] G. Porte, R. Gomati, O. El Haitamy, J. Appell, J. Marignan, J. Phys. Chem. 90 (1986) 5746.
[40] T.J. Drye, M.E. Cates, J. Phys. Chem. 96 (1992) 1367.
[41] Y. Bohbot, A. Ben-Shaul, R. Granek, W.M. Gelbart, J. Chem. Phys. 103 (1995) 8764.
[42] Z. Lin, Langmuir 12 (1996) 1729.
[43] A. Bernheim-Groswasser, E. Wachtel, Y. Talmon, Langmuir 16 (2000) 4131.
[44] T. Tlusty, S.A. Safran, J. Phys. Condens. Matter 12 (2000) 1.
[45] S. May, Y. Bohbot, A. Ben-Shaul, J. Phys. Chem. B 101 (1997) 8648.